Effect of the shaft roughness on the performance of rotary lip seals: Hydrodynamic Model.

LAHJOUJI Imane, EL GADARI Mhammed, RADOUANI Mohammed
Research team IMSM
ENSAM, University of Moulay Ismail
Meknès, Morocco
imanelahjouji14im@gmail.com ; m.elgadari@ensam-umi.ac.ma ; m.radouani@ensam-umi.ac.ma

***Abstract*—Most of the numerical studies of rotary lip seal are performed by considering lip or shaft as smooth surfaces. Although this assumption is far from practice, it is, the best approach to avoid the transient term of Reynolds equation.**

In the present work, Reynolds equation was resolved by taking into account: the roughness of the both surfaces and also the cavitation effect. In order to investigate the shaft roughness effect, an implicit with "finite differences" was used. A comparison was made between results of the current numerical results and the finite volume method published in the international literature.

Numerical simulations show that the shaft roughness affects significantly the friction torque, the leakage and the load support of the lip seal.

Key-words—Hydrodynamic lubrication; roughness; Reynolds equation; finite differences; leakage rate; friction torque

I. INTRODUCTION

The lip seals are the dynamic sealing device the most used in the industry. Since the seventies, it has been shown that under steady state conditions, a lubricating film separates the lip and the shaft surfaces.

Numerically and experimentally, it has been proved that the asperities of the shaft and lip produce a hydrodynamic force that carries the lip surface. Indeed, when the liquid is moved over each asperity, the film thickness varies and produces a pressure elevation on the upstream side, and cavitation occurs on the downstream side.

The resultant of the hydrodynamic pressure in the vicinity of the asperities generates the lift force which keeps the lip separated from the shaft.

To understand the film behavior, several lubrication models were studied namely HD (Hydrodynamic) EHD (Elastohydrodynamic), TEHD (Thermo-Elastohydrodynamic), and VEHD (Visco-Elastohydrodynamic).

In the transient condition, theoretically, it is tedious to couple the thermal phenomenon to the mechanical behavior of the lip (viscoelastomeric or elastomeric law). Indeed, if assuming shaft as smooth surface predicts easily the lip performance, with rough finish, several numerical limitations are to challenge; a lot of loops are used to stabilize solutions of energy equation, thereby the lip elasticity, the lubricant viscosity and also the active and non active zones.

In this work we will investigate the effect of the shaft roughness on the rotary lip seal performance, through the HD modeling. This study resolves Reynolds equation [1] in the active and non-active zone by taking into the consideration the lip and shaft roughness.

A numerical analysis of the isothermal hydrodynamic lubrication was performed by using the implicit temporal scheme and the finite difference spatial method. The purpose of this paper is to identify the parameters related to shaft roughness that affects the lip seal life expectancy: hydrodynamic force, friction torque, leakage rate and to compare the results with those of Shen [2].

II. MODEL USED

The lip seal and the sealing zone are shown in Figure 1. The rotating shaft is considered rough, and the lip seal is aligned [3]. In the practice, the ratio of width contact between lip and shaft by the perimeter is about 10^{-6}. Such weak domain induces numerical difficulty to mesh and resolve Reynolds equation. In order to avoid this limitation a cyclic cell is considered. Indeed, the lip roughness is periodically distributed along the «x-axis » direction with a circumferential wavelength equal to «L» .Therefore; we just consider a single cell having a length «L» and an axial contact width « b » and multiply the local results by cell numbers to deduce the global performances.

1. The film thickness

The film thickness between the lip seal and the shaft is computed by subtracting the lip roughness h_1, the shaft roughness h_2. Because the full film lubrication is considered, it is important to note that the average film thickness h_0 is considered so as to represent the gap separating the surfaces and also to neglect the contact between the asperities. Then, the expression of the film thickness [1] is given by (1):

$$h = h_1(x,y) - h_2(x,y,t) + h_0 \quad (1)$$

2. Fluid mechanics

The pressure field is described by Reynolds equation. The cavitation zones are assumed to be filled with a homogeneous

Xème Conférence Internationale : Conception et Production Intégrées, CPI 2015, 2-4 Décembre 2015, Tanger - Maroc.

Xth International Conference on Integrated Design and Production, CPI 2015, December 2-4, 2015, Tangier - Morocco.

lubricant-air mixture. The film thickness is smaller than the radius of the shaft therefore the shaft curvature can be neglected. The Reynolds equation (2):

$$\frac{\partial}{\partial x}\left(h^3 F \frac{\partial D}{\partial x}\right)+\frac{\partial}{\partial y}\left(h^3 F \frac{\partial D}{\partial y}\right)=6\mu U\frac{\partial h}{\partial x}+12\mu\frac{\partial h}{\partial t}+6\mu(1\text{-}F)\left(U\frac{\partial D}{\partial x}+2\frac{\partial D}{\partial t}\right) \quad (2)$$

In the active zone (3):

$$\begin{cases} D = p,\ D \geq 0 \\ F = 1 \end{cases} \quad (3)$$

In the cavitation zone (not active) (4):

$$\begin{cases} D = r\text{-}h,\ D < 0 \\ F = 0 \end{cases} \quad (4)$$

And $r = \frac{\rho h}{\rho_0}$ (5)

Where "r" is the replenishment ratio, "ρ" is the lubricant density and "ρ_0" is the air density.

TABLE I. NOMENCLATURE

Nomenclature

A_1	half amplitude of lip surface fluctuation [m]
A_2	half amplitude of shaft surface fluctuation [m]
b	width of solution space (sealing zone) in axial (y) direction [m]
D	universal variable
F	Flag indicating cavitation zones
L	length of solution space in circumferential (x) direction [m]
l_{11}	lip surface wavelength in x direction [m]
l_{12}	lip surface wavelength in y direction [m]
l_{21}	shaft surface wavelength in x direction [m]
l_{22}	shaft surface wavelength in y direction [m]
P	Pressure [Pa]
Pa	Ambient pressure [Pa]
Ps	Lubricant pressure [Pa]
Q	reverse pumping rate [g/h]
R_a	average roughness height [m]
U	speed of shaft surface [m/s]
W	load support [N]
x	axial coordinate [mm]
y	circonferential coordinate [m]
y_b	axial location of maximum circumferential shear deformation of lip [m]
μ	Viscosity [Pa·s]

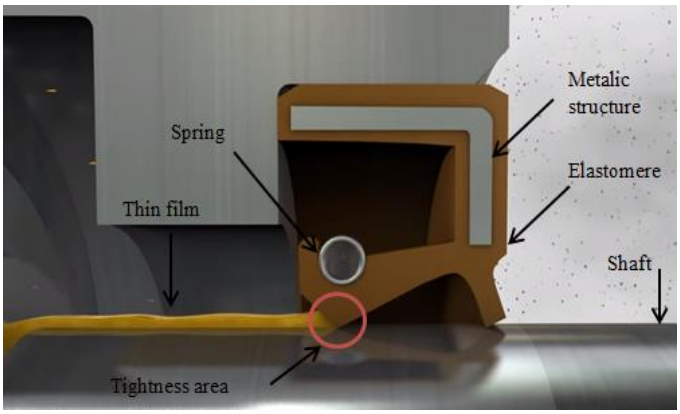

Fig. 1. Lip seal structure and location of the tightness area

III. LIP AND SHAFT ROUGHNESS

The surface roughness is considered as double sinusoidal function and the average film thickness is equal to 1μm. Thus, the lip roughness is modeled by (6):

$$h_1(x,y) = A_1 \cos\left(\frac{2\pi}{l_{11}}(x - c_g)\right)\cos\left(\frac{2\pi}{l_{12}}y\right) \quad (6)$$

where c_g is shearing deformation of the lip, with:

$$\begin{cases} c_g = l_{11}\left(\frac{2y}{y_b}\text{-}\frac{y^2}{{y_b}^2}\right) & \text{if } y < y_b \\ c_g = l_{11}\left(1\text{-}2y_b + 2y_b y\text{-}y^2\right) & \text{if } y \geq y_b \end{cases} \quad (7)$$

and y_b represents the location of the maximum dry contact pressure (results of structural analysis with the commercial simulation software « Abaqus ») as shown in Figure 2.

We assume that shaft roughness is given by:

$$h_2(x,y,t) = A_2 \cos\left(\frac{2\pi}{l_{21}}(x - t * U)\right)\cos\left(\frac{2\pi}{l_{22}}y\right) \quad (8)$$

The Reynolds equation is resolved by the finite differences method [4] using the algorithm shown in Figure 3.

As soon as the Reynolds equation is solved, the lifting load is calculated by (9), the leakage rate by (10) and the friction torque by (11).

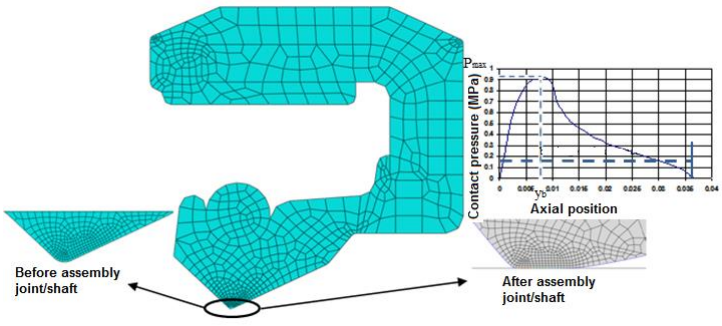

Fig. 2. The maximum circumferential strain location [1]

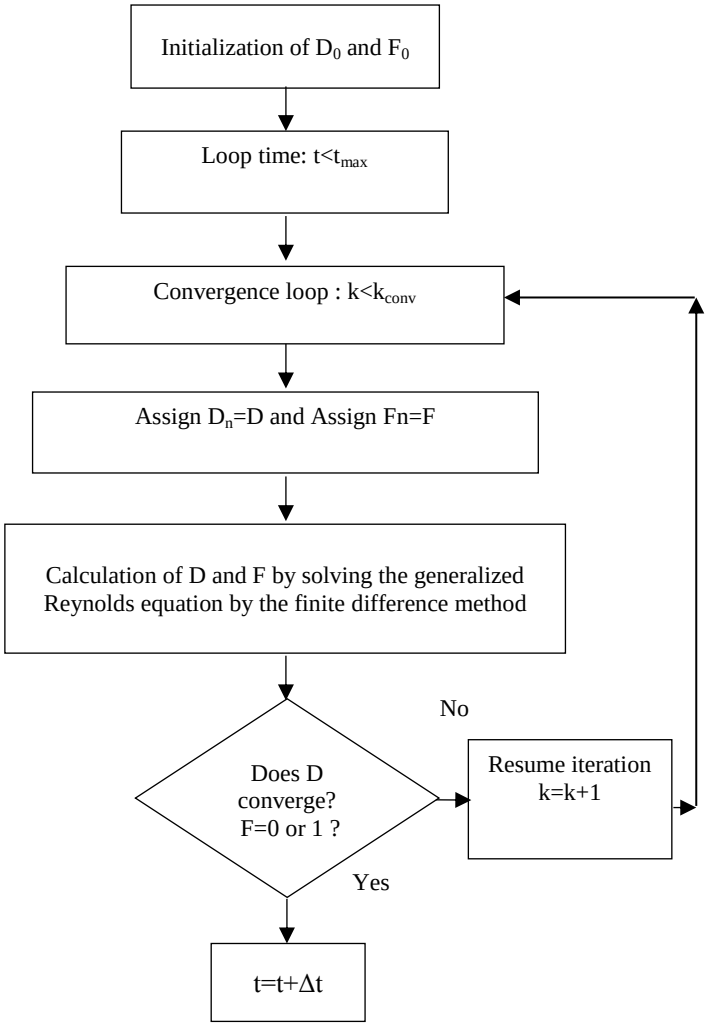

Fig. 3. Flowchart for the resolution of the Reynolds equation

$$W = \iint (p - p_a) dxdy \quad (9) \qquad Q = \int -\frac{h^3}{12}\frac{\partial p}{\partial y} \mathrm{dx} \quad (10)$$

$$C = \iint (-\frac{1}{2}\frac{\partial P}{\partial x} h + \mu \frac{U}{h}) dxdy \quad (11)$$

1. Finite Differences model

In this part the Reynolds equation is discretized using the finite difference approach.

This method employs approximations to the partial derivatives then the area of study should be mesh.

As previously cited the domain is a rectangle with "b" as length and "L" as width shown in Figure 3, thereby, we discretize cyclic cell to « (Nx-1)·(Ny-1) » regular elements. Where "Nx·Ny" nodes representing the hydrodynamic pressure. The time step is given by « Nt » partition throughout the time period.

Therefore, we discretize the terms of the partial derivative using the Taylor-Young formulation:

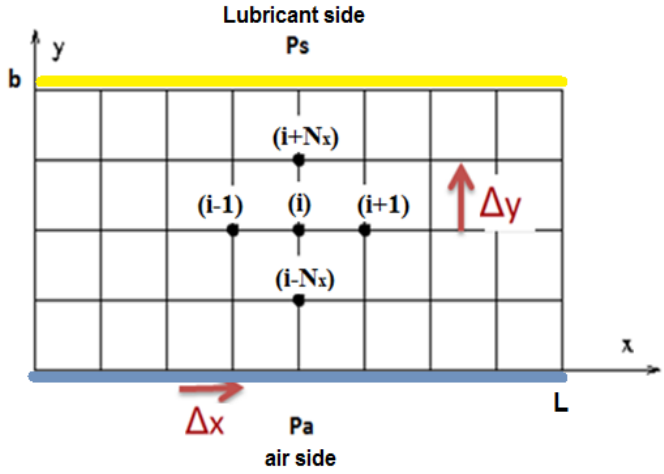

Fig. 4. Schematic representation Finite differences mesh

$$\begin{cases} \dfrac{\partial D}{\partial x} = \dfrac{D^n(i) - D^n(i-1)}{\Delta x} \\ \dfrac{\partial D}{\partial y} = \dfrac{D^n(i) - D^n(i-Nx)}{\Delta y} \\ \dfrac{\partial D}{\partial t} = \dfrac{D^n(i) - D^{n-1}(i)}{\Delta t} \end{cases} \quad (12)$$

« i » is the index of knot and « n » is the index of time.

The boundary conditions is given by: at y=0: p=pa; at y=b: p=ps.

Replacing the partial derivatives in Eq. 2 by their finite difference analogs given in Eq. 12, it yields:

$$-A \cdot D^n(i) + B \cdot D^n(i+1) + C \cdot D^n(i-1) + E \cdot D^n(i+Nx) + F \cdot D^n(i-Nx) = G + H \cdot D^{n-1}(i) \quad (14)$$

Where:

$$A = \frac{\left(2{h_n}^3(i) + {h_n}^3(i+1) + {h_n}^3(i-1)\right) F^n(i)}{2\Delta x^2} + \frac{\left(2{h_n}^3(i) + {h_n}^3(i+Nx) + {h_n}^3(i-Nx)\right) F^n(i)}{2\Delta y^2} + \frac{12\mu\left(1 - F^n(i)\right)}{\Delta t}$$

$$B = \frac{\left({h_n}^3(i+1) + {h_n}^3(i)\right) F^n(i+1)}{2\Delta x^2} - 6\mu U \frac{\left(1 - F^n(i+1)\right)}{2\Delta x}$$

$$C = \frac{\left({h_n}^3(i) + {h_n}^3(i-1)\right) F^n(i+1)}{2\Delta x^2} - 6\mu U \frac{\left(1 - F^n(i-1)\right)}{2\Delta x}$$

$$E = \frac{\left({h_n}^3(i+Nx) + {h_n}^3(i)\right) F^n(i+Nx)}{2\Delta y^2}$$

$$F = \frac{\left({h_n}^3(i) + {h_n}^3(i - Nx)\right) F^n(i + Nx)}{2\Delta y^2}$$

$$G = 6\mu U \frac{h(i+1) - h(i-1)}{2\Delta x} + 12\mu \frac{h^{n+1}(i) - h^n(i)}{\Delta t}$$

$$H = \frac{12\mu(1 - F^{n-1}(i))}{\Delta t}$$

The linear system is transformed to matrix formulation: [M].D + R={0}, where [M] is stiffness matrix given by A, B, C, E and F and [R] is second right member.

In order to find the vector [D^n] the second part of the (Eq15) is multiplied by the reverse of the pentadiagonal matrix [A (i, n)]. Then we conclude the pressure values: if « D^n (i) » is positive the pressure « P^n (i) » takes the value of « D^n (i) » if not the pressure is nil since it's the cavitation pressure. At this time we start computing the load support, the reverse pumping rate and the friction torque by the expressions given above (Eq.9, 10 and 11).

IV. VALIDATION CODE

The problem parameters are $b=0.5.10^{-4}$ m, $L=0.5.10^{-4}$ m, $\mu= 2.5.10^{-2}$ Pa·s, $ps=1.02.10^5$ Pa, pa= $ps=1.02.10^5$ Pa, $A_1=0.5.10^{-6}$ m, $l_{11}=b$, $l_{12}=L$, $l_{22}=b/2$, $l_{21}=L/2$, $y_b=3b/4$. A parametric study was made; in order to determinate the nodes number according to x-axis and y-axis. Indeed, by choosing Nx=30 and Ny=30 the numerical results are stabilized.

The results are computed with program set on the calculation software Matlab. To validate our numerical study, the formulation in finite volumes supplied by Shen [2], was compared to the current model.

Figure.5 represents the variation of time averaged load support divided by W_0 (the time averaged load support for a smooth shaft surface during a period) according to the variation of roughness of the shaft surface. We notice that when Ra(shaft) is 5% of Ra(lip), the load support rises significantly by 25% and even if we increase the shaft roughness Ra(shaft) the load support stills considerable in comparison with the one of the smooth shaft.

Figure.6 shows the variation of the reverse pumping rate according to the variation of roughness .When Ra(shaft) is 5% of Ra(lip) the reverse pumping rate is increased by 13.5% above Q_0 (the reverse pumping rate for a smooth shaft surface), and even if we increase the shaft roughness Ra(shaft) the reverse pumping rate stills significant in comparison with the one of the smooth shaft.

We can also say that the roughness of the shaft has an effect on the time-averaged reverse pumping rate.

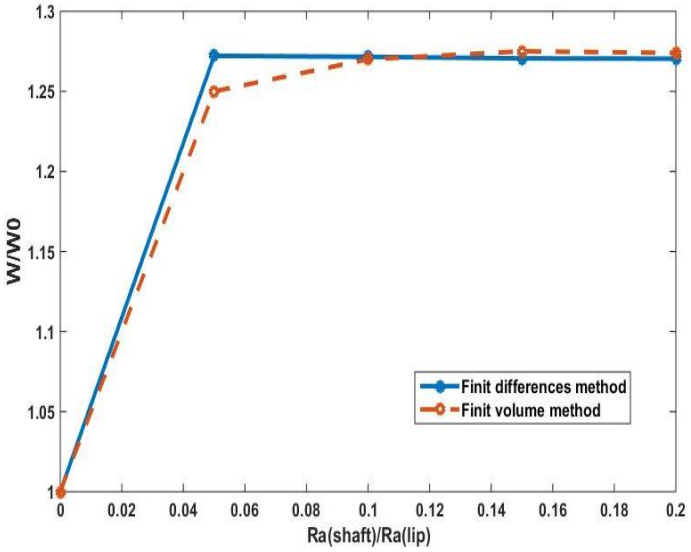

Fig. 5. Effect of Shaft Surface on Load Support

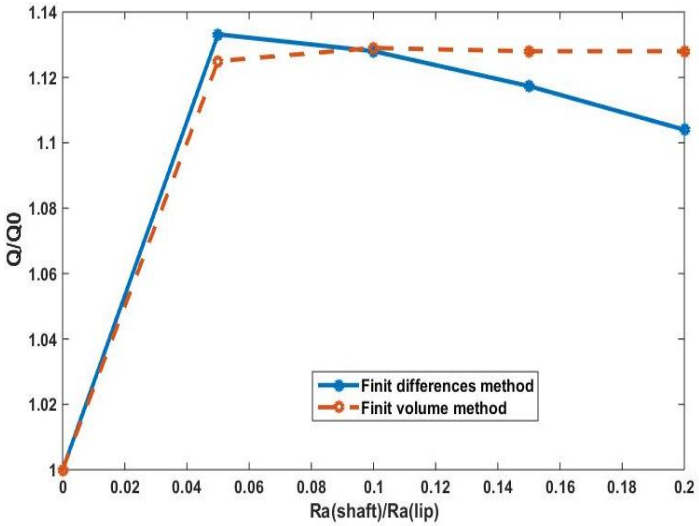

Fig. 6. Effect of Shaft Surface on Reverse Pumping Rate

The numerical results predict well the rotary lip performance comparing to finite volumes method given by Shen [2]. The differences are about 0.36% for the load support and 1.56% for the reverse pumping rate curve, as shown in figure.4 and figure.5. Thus, the current model is validated.

In order to study the effect of shaft roughness on rotary lip seal performance, we consider two influencing parameters: the roughness shape and the wavelength according to x-axis and y-axis.

V. EFFECT OF THE SHAFT ROUGHNESS

1. *Effect of the shaft surface wavelength l_{21} and l_{22}*

This part is about taking different cases of the shaft surface wavelengths, and presenting the variation of the load support and the reverse pumping rate in function of time.

Figure.7 shows that by increasing « l_{21} » the averaged lifting load and reverse pumping fall.

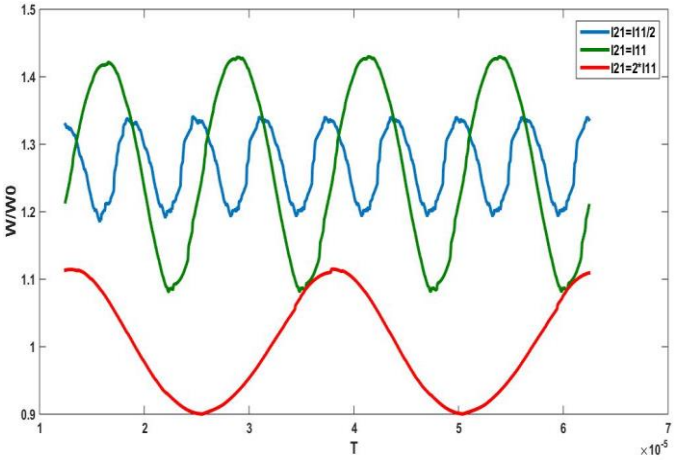

Fig. 7. Effect of Shaft Surface wave length in x direction on load support

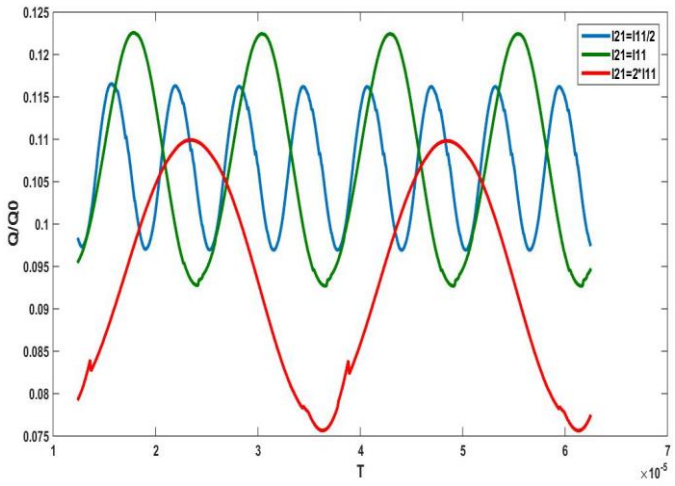

Fig. 8. Effect of Shaft Surface wave length in x direction on pumping rate

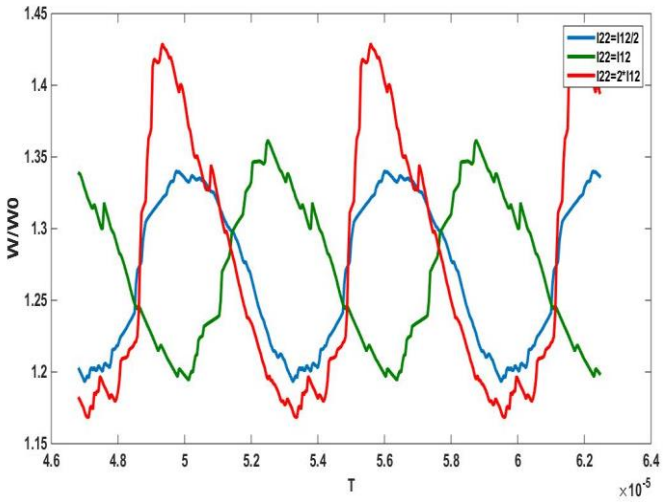

Fig. 9. Effect of Shaft Surface wave length in y direction on load support

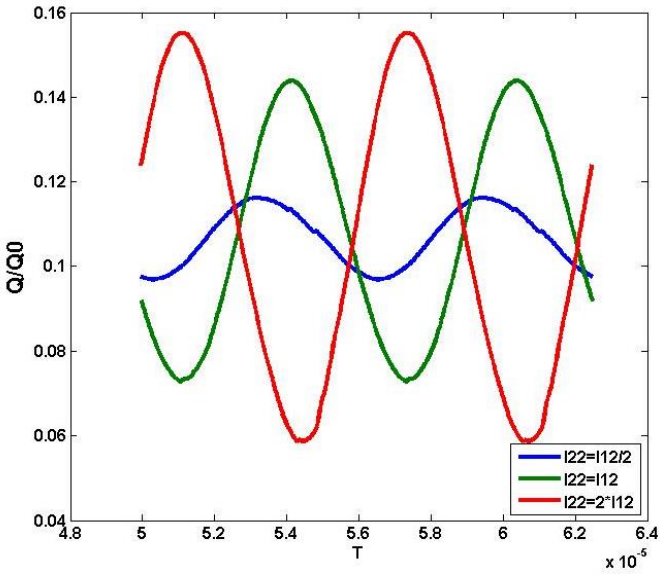

Fig. 10. Effect of Shaft Surface wave length in y direction on pumping rate

However, while changing the values of the shaft surface wavelength according to the "y" direction « l_{22} » », it is observed that the amplitude of load and reverse pumping are significantly increased and the averaged results are similar.

Thus, the effect of the shaft surface wavelength according to the x direction « l_{21} » reduces the averaged reverse pumping rate and the load support though « l_{22} » fluctuates more the amplitude of reverse pumping and lifting load, however the averaged values are quite the same.

2. Effect of the shaft roughness form

In order to investigate the effect of shaft roughness shape, we consider three cases as shown in figure.11:

- SH#1: $h_{21}=h_2(x,y,t)$ given by equation (8)
- SH#2: $h_{22}=(|h_{21}(x,y,t)|+ h_{21}(x,y,t)))/2$
- SH#3: $h_{23}=(-|h_{21}(x,y,t)|+ h_{21}(x,y,t)))/2$

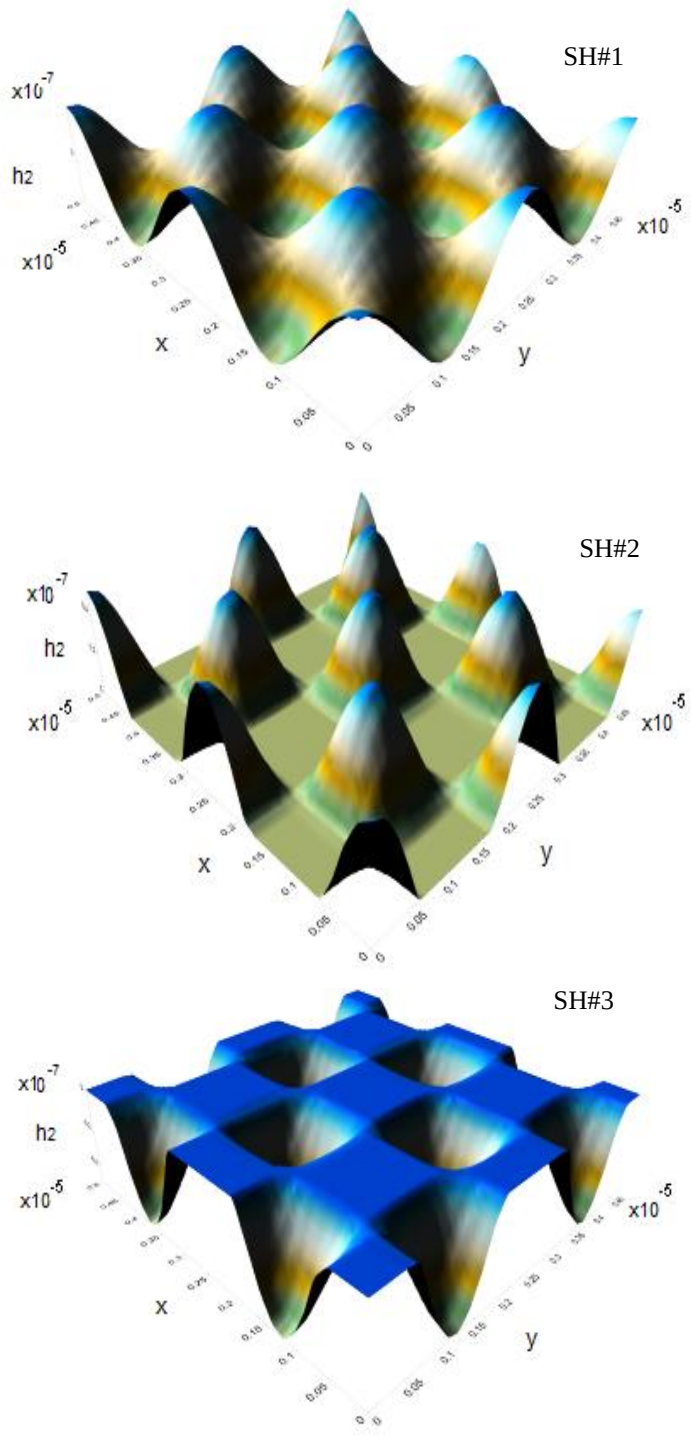

Fig.11. Shaft surface roughness profile

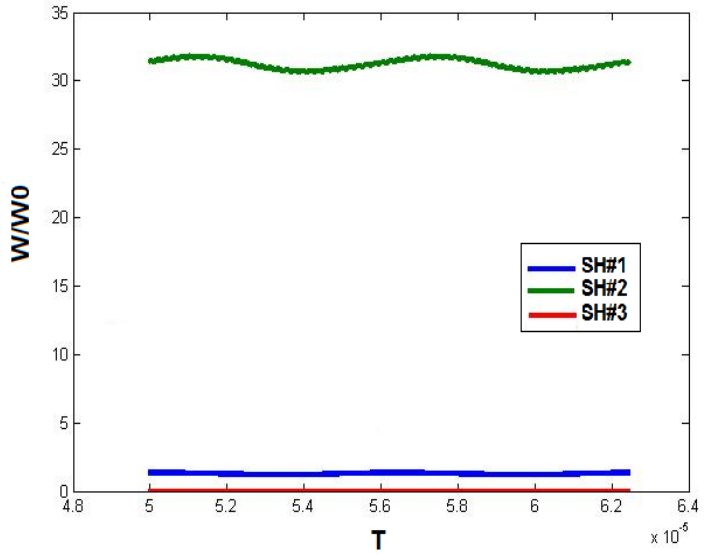

Fig.12. Effect of Shaft Surface form on the load support

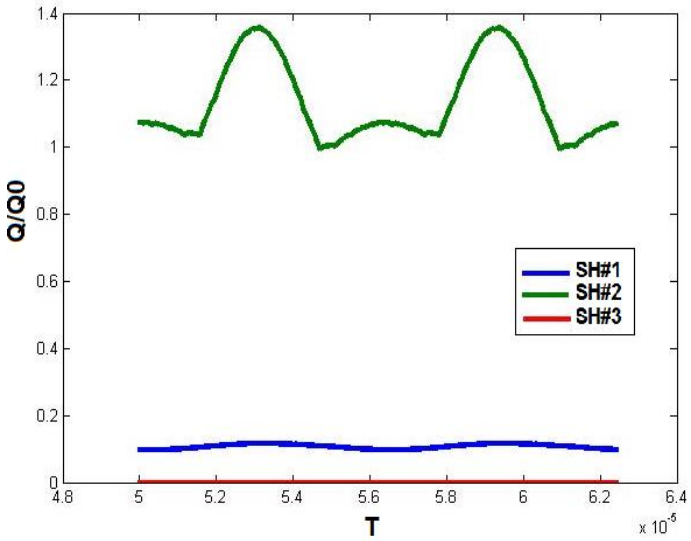

Fig. 13. Effect of Shaft Surface form on the pumping rate

For the second case we find that it raises both the load support and the reverse pumping rate contrary to the third case wish reduces the two parameters to 0.

3. Effect of the shaft roughness on the friction torque

The curves plotted in Figure 14, show the variation of the friction torque for the different cases mentioned below. It is remarkable that the shaft surface form or wavelengths fluctuations have the same effects, found for the load support or the reverse pumping rate, on the friction torque « C ».

- SH#1: $l_{21}=l_{11}/2$ and $l_{22}=l_{12}/2$
- SH#2: $h_{22}= (|h_{21}(x,y,t)|+ h_{21}(x,y,t)))/2$
- SH#3: $h_{23}= (-|h_{21}(x,y,t)|+ h_{21}(x,y,t)))/2$

- SH#4: $l_{21}=l_{11}$and $l_{22}=l1_2/2$
- SH#5: $l_{21}=2.l_{11}$ and $l_{22}=l_{12}/2$
- SH#6: $l_{21}=l_{11}/2$ and $l_{22}=l_{12}$
- SH#7: $l_{21}=l_{11}/2$ and $l_{22}=2.l_{12}$

4. Numerical simulation

The curves figured in figure.15 show the Hydrodynamic pressure plotted in function of the x and y coordinates, for different cases studied previously with an average film thickness h_0=3 µm. The curves are elaborated on the golden software surfer 9.

While changing the shaft surface wavelengths it is noticed that the pressure varies feebly. However, if the shaft surface form varies: for SH#2 the pressure rises significantly and the cavitation zone is smaller than the other cases, besides for SH#3 the cavitation zone is enormous which allow as to conclude that in this case the shaft and the lip are no more separated so this case should be avoided for a better use of the lip seal.

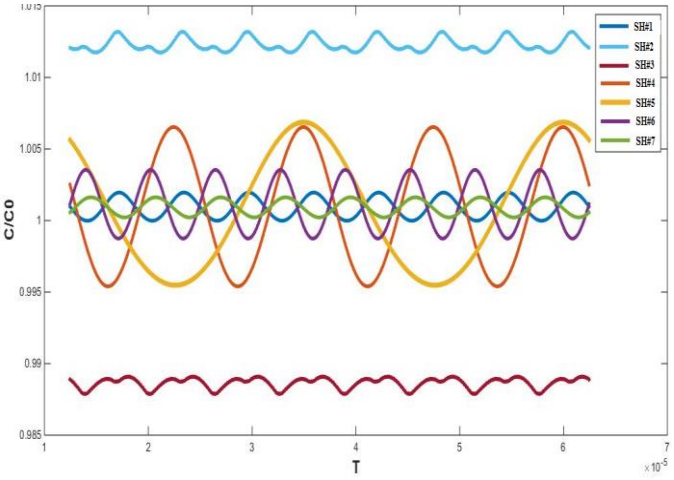

Fig. 14. Effect of Shaft Surface form on the pumping rate

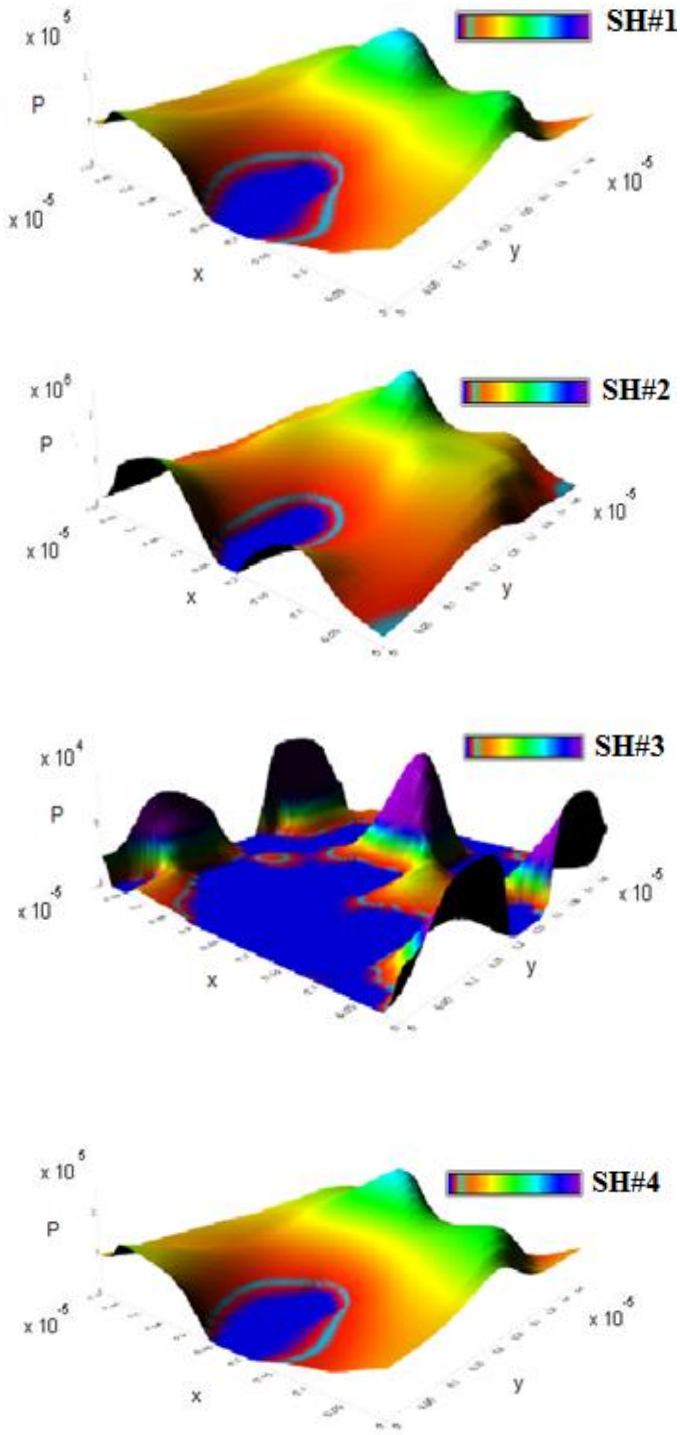

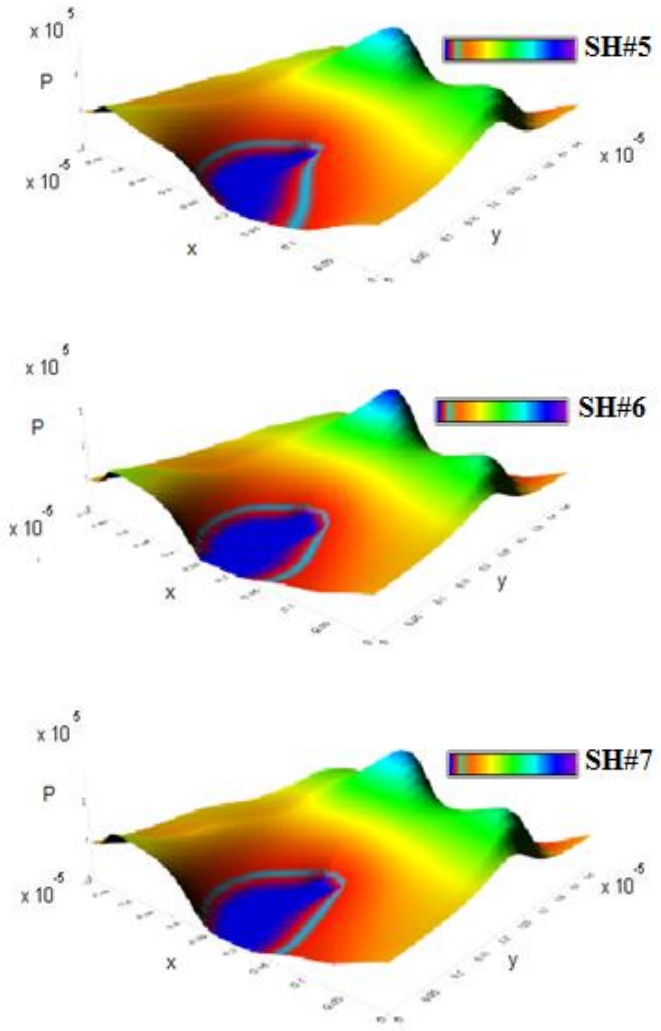

Fig. 15. Hydrodynamic pressure distribution (3D model)

VI. CONCLUSION

This work has twofold objectives, in one hand to compare numerical results between the finite differences and the volume differences approaches, in order to resolve Reynolds equation. This study confirms an accordance of the current model and the results published in the international literature.

In the other hand, this work underlines the effect of shaft roughness on rotary lip seal performance. The simulations show that the wavelength according to "x-axis" decreases the reverse pumping rate, the load support and the friction torque. Nevertheless, the wavelength according to "y-axis" rises these parameters.

In the same time, the shaft surface form has a great effect on lip seal behavior. Effectively, while taking only the positive bumps the reverse pumping rate, the load support and the friction torque rise significantly, yet if we consider only the negative bumps the parameters reduce and even approaches zero. Similarly, for the pressure distribution, while changing the shaft shape, the pressure decreases for the negative bumps however it raises significantly for the positive bumps.

REFERENCES

[1] M.El Gadari "Étude expérimentale et numérique du comportement des joints à lèvre," Soutenue le 04 décembre 2013 à l'Univérsité Hassan II.

[2] D. Shen, "Deterministic modeling of a rotary lip seal with microasperities on the shaft surface," Presented at the Académique University, Georgia Institute of Technology ,Decembre 2005.

[3] A.Maoui, M.Hajjam, D.Bonneau "Effect of 3D lip deformations on elastohydrodynamic lip seals behaviour,"ScienceDirect, Tribology International 41(2008)901-907,Fevrier 2008

[4] J. Kouatchou, "Finite Differences and Collocation Methods for the solution of two dimensional," NASA Goddard Space Flight Center,Code 931,Greenbelt,MD 20771.